THE JOURNAL OF BIOLOGICAL CHEMISTRY VOL. 289, NO. 9, pp. 5758–5773, February 28, 2014

Protein Disulfide Isomerase Directly Interacts with β-Actin Cys^{374} and Regulates Cytoskeleton Reorganization*

Received for publication, December 18, 2013 Published, JBC Papers in Press, January 10, 2014, DOI 10.1074/jbc.M113.479477

Katarzyna Sobierajska[‡], Szymon Skurzynski[‡], Marta Stasiak[‡], Jakub Kryczka[‡§], Czeslaw S. Cierniewski[‡§1], and Maria Swiatkowska[‡2]

From the [‡]Department of Molecular and Medical Biophysics, Medical University of Lodz, 92-215 Lodz, Poland and the [§]Institute of Medical Biology, Polish Academy of Sciences, 93-232 Lodz, Poland

Background: PDI regulates cytoskeleton reorganization by the thiol-disulfide exchange in β-actin.
Results: PDI directly binds to Cys^{374} of β-actin during cell adhesion and spreading.
Conclusion: Interaction of PDI with β-actin is induced by integrin-mediated cell adhesion and promotes cytoskeleton reorganization.
Significance: PDI is a new regulator of the intramolecular disulfide-thiol rearrangement of β-actin in response to αIIbβ3 integrin engagement.

Recent studies support the role of cysteine oxidation in actin cytoskeleton reorganization during cell adhesion. The aim of this study was to explain whether protein disulfide isomerase (PDI) is responsible for the thiol-disulfide rearrangement in the β-actin molecule of adhering cells. First, we showed that PDI forms a disulfide-bonded complex with β-actin with a molecular mass of 110 kDa. Specific interaction of both proteins was demonstrated by a solid phase binding assay, surface plasmon resonance analysis, and immunoprecipitation experiments. Second, using confocal microscopy, we found that both proteins colocalized when spreading MEG-01 cells on fibronectin. Colocalization of PDI and β-actin could be abolished by the membrane-permeable sulfhydryl blocker, *N*-ethylmaleimide, by the RGD peptide, and by anti-αIIbβ3 antibodies. Consequently, down-regulation of PDI expression by antisense oligonucleotides impaired the spreading of cells and initiated reorganization of the cytoskeleton. Third, because of transfection experiments followed by immunoprecipitation and confocal analysis, we provided evidence that PDI binds to the β-actin Cys^{374} thiol. Formation of the β-actin-PDI complex was mediated by integrin-dependent signaling in response to the adhesion of cells to the extracellular matrix. Our data suggest that PDI is released from subcellular compartments to the cytosol and translocated toward the periphery of the cell, where it forms a disulfide bond with β-actin when MEG-01 cells adhere via the αIIbβ3 integrin to fibronectin. Thus, PDI appears to regulate cytoskeletal reorganization by the thiol-disulfide exchange in β-actin via a redox-dependent mechanism.

Actin, a major component of the cytoskeleton, is involved in multiple cellular functions such as proliferation, adhesion, motility, growth, and cytokinesis. It belongs to the most important targets of integrin-mediated signaling (1). Recent studies showed that its intracellular activity is directly regulated by reactive oxygen species (2). The β-actin molecule contains six conserved cysteine residues, but only one of them, located at position 374, is exposed on the surface of the molecule (3, 4). This cysteine residue takes part in actin polymerization as well as in filament formation (5). Both processes are preceded by the intracellular oxidation of β-actin, which results in the formation of the disulfide bond between the sulfhydryl group Cys^{374} and glutathione (4). The oxidative modifications of β-actin play a key role in the GSH disulfide formation upon integrin engagement and cell spreading. The glutathionylation of β-actin that occurs during cell adhesion leads to the disassembly of actomyosin filaments (2). On the other hand, oxidation of β-actin creates intermolecular disulfide bonds between Cys^{374} residues of neighboring β-actin molecules and thus prevents β-actin polymerization (6). In consequence, it leads to a cytoskeleton rearrangement (7, 8).

The activity of redox-sensitive proteins is usually regulated by enzymes belonging to the glutaredoxin and thioredoxin systems, which convert disulfide bond cross-linked proteins back to their forms containing free sulfhydryl groups (9, 10). In this report, we attempted to evaluate the role of PDI[3] in the regulation of cellular β-actin activity. PDI, a member of the thiol-disulfide oxidoreductase family, displays thiol isomerase, oxidase, and reductase activity. The canonical function of PDI is a disulfide bond formation in the nascent protein and protein folding in the endoplasmic reticulum (11). PDI has multiple biological functions and interacts with numerous proteins (12). Extracellular PDI is known to mediate platelet aggregation and thrombus formation (13, 14). After activation of the platelets and endothelial cells, it can be found both inside and outside of the cells, in association with F-actin microfilaments or with cellular membranes, respectively (14–18).

* This work was supported by Project N401 140939 from the Polish National Science Center (to M. S.).
[1] Supported by Project 2011/02/A/NZ3/00068 from the National Science Center.
[2] To whom correspondence should be addressed: Dept. of Molecular and Medical Biophysics, Medical University of Lodz, 6/8 Mazowiecka St., 92-215 Lodz, Poland. Tel.: 48-42-2725721; Fax: 48-42-2725730; E-mail: maria.swiatkowska@umed.lodz.pl.

[3] The abbreviations used are: PDI, protein disulfide isomerase; NEM, *N*-ethylmaleimide; TRITC, tetramethylrhodamine isothiocyanate; FRET-AP, Forster resonance energy transfer acceptor photobleaching.

In this report, we show that PDI, through binding to β-actin-CYA, affects the thiol exchange mechanism during the adhesion of cells to fibronectin. Our data provide evidence that PDI catalyzes the thiol-disulfide exchange reaction in β-actin-CYA during cell adhesion and that it is a major enzyme responsible for redox regulation of the cytoskeleton rearrangement.

EXPERIMENTAL PROCEDURES

Reagents—All standard tissue culture reagents including RPMI 1640 medium, fetal bovine serum, Lipofectamine 2000, Opti-MEM, and Gene Tailor site-directed mutagenesis system reagent, plasmid pRSETa, and BL21Star (DE3) *E. coli* were obtained from Invitrogen. Plasmid pGEFP-N1 was from Clontech. TriPure reagent was from Roche Diagnostics. All primers were produced by Genomed (Warsaw, Poland). Moloney murine leukemia virus reverse transcriptase (M-MLV RT) and the Wizard Miniprep kit for isolated DNA were purchased from Promega Corp. (Madison, WT). Protein A/G-agarose, ECL Western blotting substrate, mouse monoclonal PDI-antibody (RL90), subcellular protein fractionation kit for cultured cells, NE-PER nuclear and cytoplasmic extraction reagents, and the BCA protein assay kit were from Thermo-Pierce. Anti-αIIbβ3 antibody (ab662) was from Abcam (Cambridge, UK). Mouse monoclonal anti-β-actin-CYA and anti-γ-actin-CYA antibody were a gift from Prof. Christine Chaponnier (Department of Pathology and Immunology Centre Medical Universitaire, University of Geneva, Switzerland). Goat anti-mouse antibodies, goat anti-rabbit antibodies, and anti-β-actin antibodies (I-19) conjugated with horseradish peroxidase were purchased from Santa Cruz Biotechnology (Santa Cruz, CA). Nonmuscle human platelet actin was from Cytoskeleton Inc. (Denver, CO). All other reagents, except where noted, were from Sigma.

Cell Culture—Megakaryocyte cell line (MEG-01) was cultured as described previously (19). The cells were grown in plastic tissue culture flasks in an RPMI 1640 medium containing 2 mM L-glutamine supplemented with 20% fetal calf serum (v/v), 100 units/ml penicillin, and 0.1 mg/ml streptomycin. The cells were cultured at 37 °C in a humidified atmosphere of 5% CO_2 and maintained at a count of between 0.5 and 1.0×10^6 cells/ml.

Cell Adhesion Assays—Adhesion of MEG-01 cells was tested using 96-well plates coated with fibronectin (10 μg/ml) and blocked with 1% BSA in PBS at 37 °C in a humidified 5% CO_2 atmosphere. Cells that were preincubated with a selected factor or nontreated were harvested, washed with PBS, and resuspended in adhesion buffer (FCS-free growth medium RPMI 1640 containing 0.5% BSA, 1 mM $CaCl_2$, 1 mM $MgCl_2$). The cells were plated (2.5×10^4/well) in wells containing 100 μl of adhesion buffer and allowed to attach for 0, 0.5, 1.0, and 2.0 h. Then they were washed gently three times with adhesion buffer to remove any nonadherent cells. The number of adherent cells was determined with the CyQuant proliferation assay kit (Invitrogen). Before the experiments, the cells were preincubated with tested reagents, such as *N*-ethylmaleimide (10 mM), cyclic RGD (1 mM), cyclic RGE (1 mM), or anti-αIIbβ3 antibodies (20 μg/ml) for 30 min at 37 °C in a humidified 5% CO_2 atmosphere and then placed on fibronectin-coated wells.

Confocal Microscopy—For a microscopic examination, the MEG-01 cells (0.5×10^6 cells/ml) were, before and after transfection with pEGFP-β-actin or its mutant pEGFP-β-$actin_{C374A}$, placed on sterile glass microscope slides that had been precoated either with fibronectin or poly-L-lysine. After incubation for 0.5, 1.0, and 2.0 h, any nonadherent cells were removed by washing with PBS, and adherent cells were fixed with 4% formaldehyde in PHEM buffer (60 mM Pipes, pH 6.9, containing 25 mM Hepes, 10 mM EGTA, 4 mM $MgCl_2$, and protease inhibitors such as 1 mM PMSF, 0.1 mM EDTA, 1 mM leupeptin, and 1 mg/ml aprotinin) for 20 min at room temperature, then washed three times with PHEM buffer, and permeabilized with 0.1% Triton X-100 (v/v). The slides were then blocked with 2% BSA in PHEM buffer for 60 min at room temperature. Endogenous PDI and β- or γ-actin were detected in the untransfected cells with a polyclonal antibody specific to PDI (5 μg) conjugated with TRITC or a mouse monoclonal to β-actin-CYA-FITC, or γ-actin-CYA-CY5.5, at 37 °C. To minimize cross-talk between the fluorochromes, the fluorescent signals were acquired sequentially at excitation wavelengths of 488, 546, and 633 nm. The confocal laser microscope Leica TCS SP5 system was used at the Laboratory of Confocal Microscopy in the Nencki Institute of Experimental Biology for intracellular probe visualization. Series of single 0.2-μm optical sections were collected. The images were scanned at high resolution (×63 oil objective, 1.4 NA). Colocalization of proteins was quantified by calculating Mander's overlap coefficient (*R*), ranging from 0 (minimum colocalization degree) to 1 (maximum colocalization degree) in digital images using Leica Application Suite software.

Forster Resonance Energy Transfer—To study the direct interactions of proteins that appeared to colocalize in immunocytochemical assays *in vivo*, a confocal microscopy-based FRET acceptor photobleaching (FRET-AP) method was used. Energy transfer was calculated as the percentage of the increase in fluorescence intensity of the donor (TRITC or Cy5.5, respectively) after photobleaching of the acceptor (FITC or TRITC) in a chosen region of the cell with a high intensity laser light. Estimation of donor fluorescence intensity before (*I*Dpre) and after (*I*Dpost) complete acceptor photobleaching allows the quantification of E_{eff} as follows: $E_{eff} = 1 - I\text{Dpre}/I\text{Dpost}$, $I\text{Dpost} > I\text{Dpre}$.

For the FRET-AP assay, a Leica TCS SP5 confocal microscope (Leica Microsystems GmbH, Wetzlar, Germany) operating with a white laser (between 610 and 660 nm) of 30 milliwatts, argon laser of 40 milliwatts, and a HeNe laser of 1.2 milliwatts was applied. The FRET-AP couple used in this study was an FITC fluorophore or TRITC fluorophore, respectively, as the donor and TRITC or Cy5.5 fluorophore, respectively, as the acceptor with the Forster radius in the range of 45–50 Å. Cells were examined with a 63×, 1.4 NA Leica oil immersion objective. Photobleaching of the acceptor was performed with five sequential illuminations (five frames, 2048 × 2048 resolution, line average 1, laser power 100%) of the region of interest (ROI). To excite molecules before and after bleaching, the laser line of 488 or 546 nm was used (20%). During bleaching the laser line of 546 or 633 nm (100%) was used to scan a smaller region in the cell compartments of interest. To acquire donor fluorescence, the donor channel from 500 to 540 nm or from 450 to

490 nm (donor emission intensity peak of ~520 or 480 nm) was opened, and fluorescence from 590 to 630 nm or from 500 to 540 nm (acceptor emission intensity peak ~600 nm) was collected for the acceptor channel. For spectral analysis, excitation at 488 nm was used, and the fluorescence ranging from 500 to 700 nm (10 nm steps) before and after bleaching was collected.

Construction of β-Actin and Its Mutant Fused with EGFP—To express β-actin, total RNA was isolated from the MEG-01 cells with the use of TriPure reagent, and it was reverse transcribed by using the Moloney murine leukemia virus reverse transcriptase according to the manufacturer's instructions. The resulting cDNA was a template for amplification of the full-length gene of mature β-actin. A human β-actin sequence was amplified by PCR with *Pfu* polymerase using primers containing EcoRI and BamHI site, respectively, and cloned into the pEGFP-N1 vector (a forward primer, ACGGAATTCTGATGGATGATGATATCGC, and a reverse primer, TATGGATCCCGGAAGCATTTGCGGTG). The pEGFP-β-actin$_{C374A}$ mutant was produced using the GeneTailor Site-Directed Mutagenesis System, and TCCATCGTCCACCGCAAAGCATTCTAGGAATTC and TTTGCGGTGGACGATGGAGGGGCCGGA as primers, propagated in *E. coli*, were purified with Wizard Midiprep (Promega) and sequenced to confirm the open reading frame.

Transfection of Cells—MEG-01 cells were transfected with pEGFP-β-actin or its mutant pEGFP-β-actin$_{C374A}$ using Lipofectamine 2000. A total amount of 1.5 μg of plasmid DNA and 6 μl of Lipofectamine solution was incubated for 15 min in 200 μl of Opt-MEM (Invitrogen) and then diluted with 800 μl of Opti-MEM. This solution was added to the growing MEG-01 cells in 6-well plates (Falcon, Becton Dickinson). After 6 h of incubation at 37 °C without serum, 2 ml of 10% FCS medium was added to the cells, and the medium was changed 12 h later to the RPMI 1640 medium. The yield of transfection was evaluated by analysis of fusion construct expression by fluorescence microscopy using a FITC filter set (Carl Zeiss, Jena, Germany).

Antisense phosphorothioateoligodeoxynucleotide (GGCAGCGAGACTCCGAACACGGTA) and the control with a scrambled sequence (GATGGCACAAGCCTCAGAGCGACGG) were used to silence PDI gene expression (20). Synthetic oligonucleotides (50, 100, or 200 nM) were transfected to the MEG-01 cells with Oligofectamine (Invitrogen) for 24 h at 37 °C. After transfection, the cells were gently washed and resuspended in the RPMI 1640 medium until ready for use.

Recombinant β-Actin Protein and Its Mutant—DNA coding of the β-actin sequence was amplified by PCR using the primers ACGGGATCCATGGATGATGATATCGC and TATGAATTCCTAGAAGCATTTGCGGTGGAC. Then the sequence was subcloned into BamHI and EcoRI sites in pRSETa. The pRSETa-β-actin construct was propagated in *E. coli* (BL21Star, DE3), purified with Wizard Midiprep, and sequenced to verify the integrity of the fusion protein. Cys^{374} was replaced with Ala by site-directed mutagenesis using the Gene Tailor site-directed mutagenesis system. For this purpose, the mutagenic primers TCCATCGTCCACCGCAAAGCATTCTAGGAATTC and TTTGCGGTGGACGATGGAGGGGCCGGA were used. Recombinant β-actin and β-actin$_{C374A}$ were expressed in *E. coli* transformed with pRSETa-β-actin or pRSETA-β-actin$_{C374A}$, respectively, and then incubated for 16 h at 30 °C. The harvested cells were centrifuged, resuspended in 50 mM Tris-HCl, pH 7.9, containing 2 mM EDTA, 1% Triton X-100, 1 mM PMSF, and 25 μM leupeptin, and homogenized by French press at 4 °C on ice followed by centrifugation (100,000 × *g*, 60 min, 4 °C) in binding buffer (5 mM imidazole, 150 mM NaCl, 20 mM Tris-HCl, pH 7.9) and sonicated on ice. The bacterial lysate was clarified by ultracentrifugation for 1 h at 100,000 × *g*, at 4 °C, filtered through a 0.45-μm syringe filter, and loaded onto a His-Trap column (5 ml; Amersham Biosciences) connected to an FPLC system (Amersham Biosciences). The proteins were eluted with a 5–500 mM imidazole gradient. The purity of recombinant β-actin and its mutant β-actin$_{C374A}$ was confirmed by reversed phase ultra performance liquid chromatography and by SDS-PAGE.

PDI Activity—PDI activity was evaluated on the basis of its ability to renature the denatured and reduced RNase. For this purpose RNase (30 μmol/l) was incubated with PDI (5 μmol/liter) for 24 h at room temperature. Then 10 μl of the incubation mixture was added to 200 μl of 0.44 mmol/liter cCMP dissolved in 0.1 mol/liter MOPS, pH 7.0. Changes in absorbance at 284 nm were monitored in a Unicam UV-visible spectrophotometer.

Actin Assays Using SDS-PAGE—Polymerization of recombinant β-actin protein and its mutant was determined by semi-quantitative SDS-PAGE methods that were optimized in parallel with skeletal muscle actin and platelet actin. To ensure that the experiments started with only the actin monomer, all initial actins in G-buffer (5 mM Tris-HCl, pH 8.0, 0.2 mM $CaCl_2$, and 0.2 mM ATP) were allowed to depolymerize on ice for 60 min and then were centrifuged for 30 min at 13,000 × *g* at 4 °C to sediment any remaining oligomers. Supernatants were distributed into microcentrifuge tubes, and actin polymerization buffer (500 mM KCl, 20 mM $MgCl_2$, and 10 mM ATP) was added to stimulate polymerization. Polymerization was complete after 5, 15, and 60 min, and the samples were centrifuged at 16,000 × *g* for 60 min at 25 °C to separate polymerized F-actin (pellet) from monomeric G-actin (supernatant). Samples without actin polymerization buffer were made as a control (data not shown). Both the pellet and supernatant were separated by SDS-PAGE in 12% gels. Equal volume samples (15 μl) were prepared with a sample buffer (1:1 sample to buffer ratio), loaded onto the gel, run at 150 V for 60 min, and visualized with Coomassie Blue. The developed gels were scanned, and the protein bands were quantitated by the Gel Doc 2000 gel documentation system (Bio-Rad).

Actin Cosedimentation Assay—Rabbit muscle actin was kept on ice overnight, diluted in G-buffer (to 20 μM) containing 5 mM Tris-HCl, pH 8.0, 0.2 mM $CaCl_2$, and finally incubated at room temperature for 1 h. Next, the obtained F-actin (16 μM) was mixed with PDI (2 μM), α-actinin (2 μM), and BSA (2 μM) in the following buffer: 5 mM Tris, pH 7.0, 2 mM $MgCl_2$, 0.2 mM $CaCl_2$, 50 mM KCl, 1 mM ATP, and 5 mM guanidine carbonate. As a control, a probe with only PDI was included. The reaction was incubated for 30 min at room temperature and then centrifuged at 100,000 × *g* for 30 min at room temperature. The supernatant and pellet fractions were analyzed by SDS-PAGE, and the proteins were visualized by Coomassie Blue staining.

Binding Assays—The wells of 96-well microtiter plates were coated overnight at 4 °C with PDI (5 μg/ml in PBS). Unbound proteins were washed from the wells, and nonspecific binding sites were blocked by incubation with 5% skimmed milk in PBS for 2 h at room temperature. Direct binding assay was performed by adding increasing concentrations of β-actin to immobilized PDI or to wells coated with skimmed milk. Unbound β-actin was aspirated, and the wells were washed three times with PBS containing 5% skimmed milk. β-Actin bound to PDI was detected with polyclonal rabbit antibodies specific to β-actin conjugated with horseradish peroxidase. The reaction was developed using *o*-phenylenediamine, the reaction was stopped with 4 M H_2SO_4, and a change in color was determined at 490 nm. To detect nonspecific binding, all assays were done simultaneously on plates coated with skimmed milk alone and processed as described above. The background binding to the skimmed milk was subtracted from all of the samples before data analysis.

Subcellular Fractionation of Cell Proteins—Cells were transferred to fibronectin precoated plates. Then the cells were harvested at 0.5, 1.0, and 2.0 h of incubation, rinsed with cold PBS twice, and finally centrifuged for 5 min at 400 × *g* at 4 °C. Cytoplasmic, endoplasmic reticulum, and cytoskeleton fractions were obtained using the subcellular protein fractionation kit according to the manufacturer's protocol. Finally, the fractions were separated by the SDS-PAGE method in 10% gels (21). For immunoprecipitation assay, the cytoplasm fraction was isolated by NE-PER nuclear and cytoplasmic extraction reagents to obtain nondenatured, active proteins.

Coimmunoprecipitation and Immunoblotting—For the coimmunoprecipitation experiments, lysate and cytoplasmic fraction nontreated MEG-01 cells treated with *N*-ethylmaleimide and lysate and transfected with vectors expressing β-actin or its mutant $\beta\text{-actin}_{C374A}$ were transferred to fibronectin-precoated plates. Then the cells were harvested at 0.5, 1.0, and 2.0 h of incubation, lysed in 25 mM Hepes, pH 7.5, containing 1% CHAPS, 150 mM NaCl, 5 mM $MgCl_2$, and protease inhibitors (1 mM PMSF, 0.1 mM EDTA, 1 mM leupeptin, 1 mg/ml aprotinin), and finally centrifuged for 20 min at 16,000 × *g* at 4 °C. Then the lysates were precleared with 30 μl of protein A/G-agarose bead slurry for 2 h at 4 °C to avoid nonspecific binding. Next, the protein concentration was measured by BCA. A total of 500 μg of protein from each lysate was incubated with 2 μg of anti-PDI antibodies on a rotator overnight at 4 °C. Subsequently, 100 μl of protein A/G-agarose bead slurry was added to each cell extract, and the incubation was continued for another 3 h. The beads were washed three times with PBS, suspended in 2× concentrated SDS-PAGE loading buffer, and boiled for 5 min. Proteins released from the resin were separated by SDS-PAGE in 10% gels under reducing and nonreducing conditions (22), transferred to a nitrocellulose membrane (Bio-Rad) and immunodetected by anti-β-actin-CYA, anti-γ-actin-CYA, or anti-PDI antibodies, followed by the appropriate secondary antibodies conjugated with HRP (Santa Cruz Biotechnology). Immunodetection was accomplished by using the enhanced chemiluminescence kit and Kodak BioMax light film (Eastman Kodak). The developed films were scanned, and the protein bands were quantitated by the Gel Doc 2000 gel documentation system (Bio-Rad).

Surface Plasmon Resonance Analyses—The kinetics parameters (association and dissociation rate constants, k_{on} and k_{off}, respectively) and the affinity constant (K_D) between recombinant PDI and β-actin or its mutant form were measured by surface plasmon resonance using the Biacore X system (GE Healthcare Life Sciences). The carboxymethyl dextran matrix of CM5 Sensor Chips (GE Healthcare Life Sciences) was activated by the injection (35 μl) of an 100 mM *N*-hydroxysuccinimide and 400 mM 1-ethyl-3-(3-dimethylaminopropyl) carbodiimide mixture at a 1:1 volume ratio to give reactive succinimide esters. Subsequently, PDI was covalently attached to the reactive esters of the chip via their amino groups to achieve 2000 resonance units (using a concentration of 5 μg/ml in 10 mM acetate buffer, pH 4.5, and a flow rate at 5 μl/min). The remaining active esters that were present on the chip surface were blocked by an injection of 1 mM ethanolamine HCl (35 μl). Experiments were performed at 25 °C using Hepes (150 mM NaCl, 2 mM $CaCl_2$, 0.05% (v/v), 2 mM 2 mM β-mercaptoethanol, Surfactant P20, 10 mm Hepes, pH 7.4; flow rate was 5 μl/min) as a running buffer. Different concentrations of actin or its mutant were injected (15 μl), and the amount of bound PDI to immobilized β-actin or its mutant was monitored by measuring the variation of the surface plasmon resonance angle as a function of time. The results were expressed in resonance units, which is an arbitrary unit that is specific for the Biacore X instrument (1000 resonance units corresponds to ~1 ng of bound protein/mm^2). After each injection, the sensor chip was regenerated with a short pulse (5 μl) of 10 mM glycine HCl, pH 2.5. The association rate constants, k_{on} and k_{off}, were determined separately from the individual association and dissociation phases, respectively. The overall affinity constant, K_D, was derived from k_{off}/k_{on}. All calculations were prepared with BIAevaluation 3.1 software.

Statistical Analyses—The statistical significance of the differences between the experimental conditions was determined by Student's *t* test for unpaired groups. *p* values less than 0.05 were considered significant.

RESULTS

PDI Interacts with β-Actin during Cell Adhesion and Spreading—The emerging evidence suggests that actin organizes cell adhesion and that this process can be regulated by redox mechanisms involving reactive oxygen species (2). To explain the role of PDI in the thiol-disulfide exchange occurring in the β-actin cytoskeleton during cell adhesion and spreading, in the preliminary experiments, we investigated the interaction between both proteins and the β-actin-CYA-PDI complex formation in the adhering cells. First, we assessed the location of PDI in the MEG-01 cellular fractions. For this purpose cell lysates were fractioned according to the manufacturer's protocol, and then aliquots of the cell lysates, the cytosol, membrane (containing endoplasmic reticulum proteins) and the cytoskeletal fractions were analyzed by Western immunoblotting (Fig. 1*A*). Subcellular fractionation of MEG-01 demonstrated that PDI was present mainly in the endoplasmic reticulum but that it was also observed in the cytosol and weakly in the cytoskele-

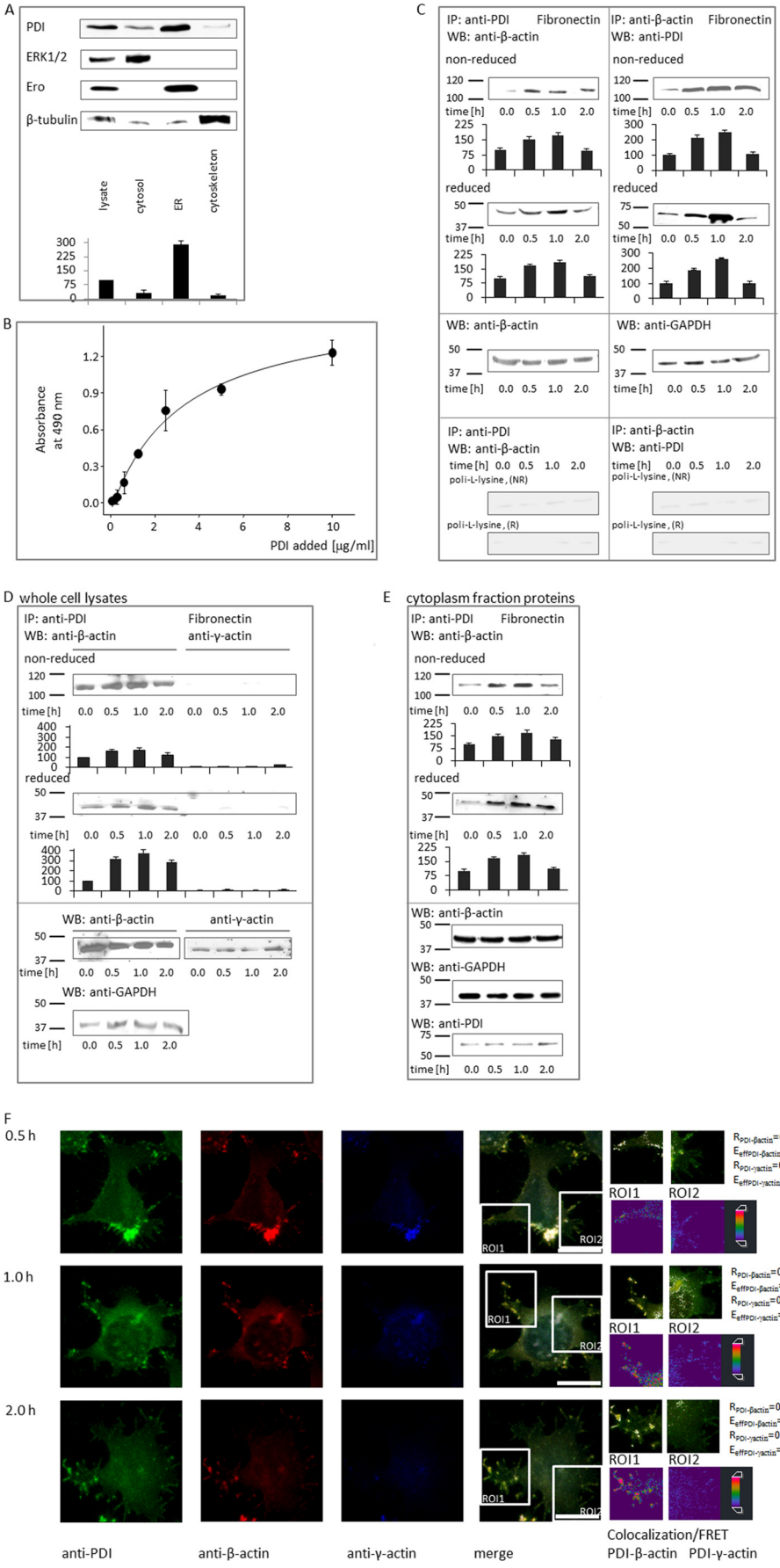
A
PDI
ERK1/2
Ero
β-tubulin
lysate
cytosol
ER
cytoskeleton
B
Absorbance at 490 nm
PDI added [μg/ml]
C
IP: anti-PDI Fibronectin
WB: anti-β-actin
IP: anti-β-actin Fibronectin
WB: anti-PDI
non-reduced
reduced
time [h] 0.0 0.5 1.0 2.0
WB: anti-β-actin
WB: anti-GAPDH
IP: anti-PDI
WB: anti-β-actin
IP: anti-β-actin
WB: anti-PDI
poli-L-lysine, (NR)
poli-L-lysine, (R)
D whole cell lysates
IP: anti-PDI
WB: anti-β-actin
Fibronectin
anti-γ-actin
non-reduced
reduced
WB: anti-β-actin
anti-γ-actin
WB: anti-GAPDH
E cytoplasm fraction proteins
IP: anti-PDI
WB: anti-β-actin
Fibronectin
non-reduced
reduced
WB: anti-β-actin
WB: anti-GAPDH
WB: anti-PDI
F
0.5 h
1.0 h
2.0 h
ROI1
ROI2
$R_{PDI\text{-}\beta actin}$=0.63±0.06
$E_{effPDI\text{-}\beta actin}$=41%
$R_{PDI\text{-}\gamma actin}$=0.21±0.02
$E_{effPDI\text{-}\gamma actin}$=1.6%
$R_{PDI\text{-}\beta actin}$=0.74±0.03
$E_{effPDI\text{-}\beta actin}$=43%
$R_{PDI\text{-}\gamma actin}$=0.24±0.02
$E_{effPDI\text{-}\gamma actin}$=2.1%
$R_{PDI\text{-}\beta actin}$=0.67±0.06
$E_{effPDI\text{-}\beta actin}$=44%
$R_{PDI\text{-}\gamma actin}$=0.23±0.03
$E_{effPDI\text{-}\gamma actin}$=1.9%
anti-PDI
anti-β-actin
anti-γ-actin
merge
Colocalization/FRET
PDI-β-actin PDI-γ-actin

ton fraction. The purity of cell fractions was monitored by Western blot analysis using an antibody that recognizes the protein markers of relevant cell fractions such as Ero, ERK1/2, and β-tubulin, respectively. Second, we searched for interaction of PDI with β-actin as analyzed by a solid phase binding assay. In this experiment, PDI was immobilized on microtiter wells, which was followed by incubation with various concentrations of β-actin. Bound β-actin was quantified using rabbit polyclonal anti-β-actin antibodies and goat anti-rabbit IgG conjugated with horseradish peroxidase as the first and second antibodies, respectively. Because is visible in Fig. 1*B*, β-actin bound to immobilized PDI in a dose-dependent manner. It neatly fit the Regression Wizard hyperbola, thus indicating the tendency to saturate. Third, we attempted to detect whether the PDI-β-actin complex can be formed in adhering cells. The MEG-01 cells were placed on fibronectin-coated dishes, collected after different time points (0, 0.5, 1.0, and 2.0 h), and subjected to immunoprecipitation (Fig. 1*C*). To study the direct interaction between PDI and β-actin-CYA, the cell extracts were incubated with mouse monoclonal antibodies specific to β-actin-CYA or rabbit polyclonal anti-PDI antibody. The obtained immunoprecipitates were separated by SDS-PAGE under reducing and nonreducing conditions, and after electrophoretic transferring onto a nitrocellulose membrane, they were blotted with monoclonal anti-β-actin-CYA or polyclonal anti-PDI antibodies, respectively. To control the concentration of cell extracts, before immunoprecipitation they were analyzed by Western immunoblotting using anti-β-actin and anti-GAPDH antibodies. Data shown in Fig. 1*C* indicate the presence of PDI in a high molecular complex with β-actin evidenced by: (*a*) an immunoprecipitate acquired through pulling down with antibodies against β-actin-CYA, blotted with anti-PDI antibodies, and (*b*) an immunoprecipitate obtained using anti-PDI antibodies blotted with antibodies against β-actin-CYA. There was a single band with a molecular mass of 110 kDa that was specifically recognized by the anti-PDI antibodies under nonreducing conditions. After reduction it showed the presence of two components, namely 65 and 45 kDa, corresponding to PDI and β-actin-CYA, respectively (Fig. 1*C*, *middle gels*). The control MEG-01 cells placed on poly-L-lysine-coated dishes did not contain such a β-actin-PDI complex. Interestingly, the formation of the β-actin-PDI complex was dependent on the time of adhesion, as evaluated by the staining intensity of the 110-kDa band. Interaction between these two proteins was most efficient after 1 h of cell adhesion to fibronectin, reaching 173% of that observed at the zero time point. It quickly decreased and approached the control values after 2 h of adhesion.

To confirm specific interaction only between PDI and β-actin-CYA, not γ-actin-CYA, the cell extracts were incubated with polyclonal anti-PDI antibody, and the immunoprecipitates were separated by SDS-PAGE as described above. Western blot assay was carried out with monoclonal anti-β-actin-CYA or anti-γ-actin-CYA antibodies, respectively. To control the protein concentration in each cell extract, before immunoprecipitation, they were analyzed by Western immunoblotting using anti-β-actin-CYA, anti-γ-actin-CYA, and anti-GAPDH antibodies. Immunoprecipitation assay followed by blotting with monoclonal anti-β-actin-CYA antibody demonstrated a single 110-kDa band under nonreducing conditions, and a 45-kDa corresponding to β-actin after reduction (Fig. 1*D*, *left panel*). For comparison, an analogous analysis with a monoclo-

FIGURE 1. **Interaction of PDI with β-actin in MEG-01 cells adhering to fibronectin.** *A*, subcellular fractionation of MEG-01 cells showed that PDI is localized in both the endoplasmic reticulum and the cytosol fraction. Equal amounts of cell lysate and cell fractions (cytosol, membrane containing endoplasmic reticulum proteins and cytoskeleton) were analyzed by Western immunoblotting using rabbit anti-PDI antibodies. In parallel, gels were blotted with antibodies specific to cellular compartment markers: rabbit anti-ERK1/2, anti-Ero, and mouse anti-β-tubulin, respectively. *B*, the interaction of β-actin with PDI as analyzed by solid phase binding assay. Interaction of both proteins was monitored using rabbit polyclonal anti-β-actin-HRP antibodies, visualized with *o*-phenylenediamine, and detected at 490 nm. Nonspecific binding was subtracted from all readings before data analysis. Each point represents the mean ± S.D. obtained in three separate experiments performed in duplicate. *C*, MEG-01 cells attached to fibronectin for 0.0, 0.5, 1.0, and 2.0 h were lysed, and the protein extracts were subjected to immunoprecipitation (*IP*) with antibodies specific to PDI or β-CYA and blotted (*WB*) with anti-β-actin-CYA or anti-PDI antibodies, respectively. In parallel, MEG-01 cells were placed on poly-L-lysine and analyzed under the same conditions (*bottom panel*). The immunoprecipitates were analyzed under nonreducing (*top gels*) and reducing (*middle gels*) conditions. The quantity of the immunoprecipitated proteins is shown below the relevant gels. For this purpose, after immunodetection using the enhanced chemiluminescence kit, the films were scanned, and the protein bands were quantitated using the Gel Doc 2000 gel documentation system (Bio-Rad). To quantify the densitometric scans, the background was subtracted, and the area for each protein peak was determined. In parallel, samples of the cell extract were blotted with control mouse IgG (not shown). Levels of β-actin-CYA and GAPDH (*bottom gels*) in each cell extract were tested before immunoprecipitation by Western immunoblotting by using specific mouse monoclonal anti-β-actin-CYA and mouse monoclonal anti-GAPDH antibodies, respectively. In addition, MEG-01 cells placed on poly-L-lysine were analyzed under the same conditions and shown as negative controls. The data are representative of three independent experiments. Additionally, to confirm specify of PDI-β-actin-CYA interaction, MEG-01 cells attached to fibronectin for 0.0, 0.5, 1.0, and 2.0 h were immunoprecipitated (*IP*) by polyclonal anti-PDI antibodies. *D*, then immunochemical assay (*WB*) with monoclonal anti-β-actin-CYA and γ-actin-CYA antibodies blotted under nonreducing (*top gels*) and reducing (*middle gels*) conditions was performed. Quantification proceeded as described previously. Levels of β-actin, γ-actin, and GAPDH (*bottom gels*) in each cell extract were tested before immunoprecipitation by Western immunoblotting by using specific mouse monoclonal anti-β-actin, anti-γ-actin, and anti-GAPDH antibodies, respectively. In addition, MEG-01 cells placed on poly-L-lysine were analyzed under the same conditions and shown as negative controls (data not shown). The data are representative of three independent experiments. Furthermore, analysis of the cytoplasm protein was done as described above. The obtained cytoplasm fraction from the MEG-01 cells attached to fibronectin for 0.0, 0.5, 1.0, and 2.0 h was treated as described in the legend to *D*. Quantification proceeded as described previously. *E*, levels of β-actin, PDI, and GAPDH (*bottom gels*) in each cell extract were tested before immunoprecipitation by Western immunoblotting by using specific mouse monoclonal anti-β-actin-CYA, anti-GAPDH antibodies, and rabbit polyclonal anti-PDI, respectively. In addition, MEG-01 cells placed on poly-L-lysine were analyzed under the same conditions and shown as negative controls (data not shown). The data are representative of three independent experiments. *F*, colocalization of β-actin or γ-actin and PDI in MEG-01 cells adhering to fibronectin was further evidenced by confocal microscopy. Representative thin section confocal fluorescence micrographs of MEG-01 cells adhering to fibronectin that were stained with PDI specific antibody conjugated with TRITC. Cells were counterstained with antibodies conjugated with FITC specific to β-actin-CYA and conjugated with Cy5.5 specific to γ-actin-CYA. Average fluorescence derived from PDI and β-actin when merged revealed extensive colocalization of these proteins, which is particularly visible in the focal adhesion sites and which increased during cell spreading in contrast to PDI to γ-actin with was very low (*enlarged sections*, *white points*). Cells, primary labeled with normal rabbit IgG, were stained with goat anti-rabbit IgG conjugated with FITC or normal mouse conjugated with TRITC or Cy5.5 antibodies and used as controls (data not shown). The Mander coefficient (*R*) was calculated from at least 20 confocal sections by Leica confocal software. FRET-AP efficiency analysis indicates an interaction between β-actin and PDI that slightly increased during cell adhesion. The increase of fluorescence intensity is converted to pseudocolor (*right panels*) that displays variations of pixel gray scales with color.

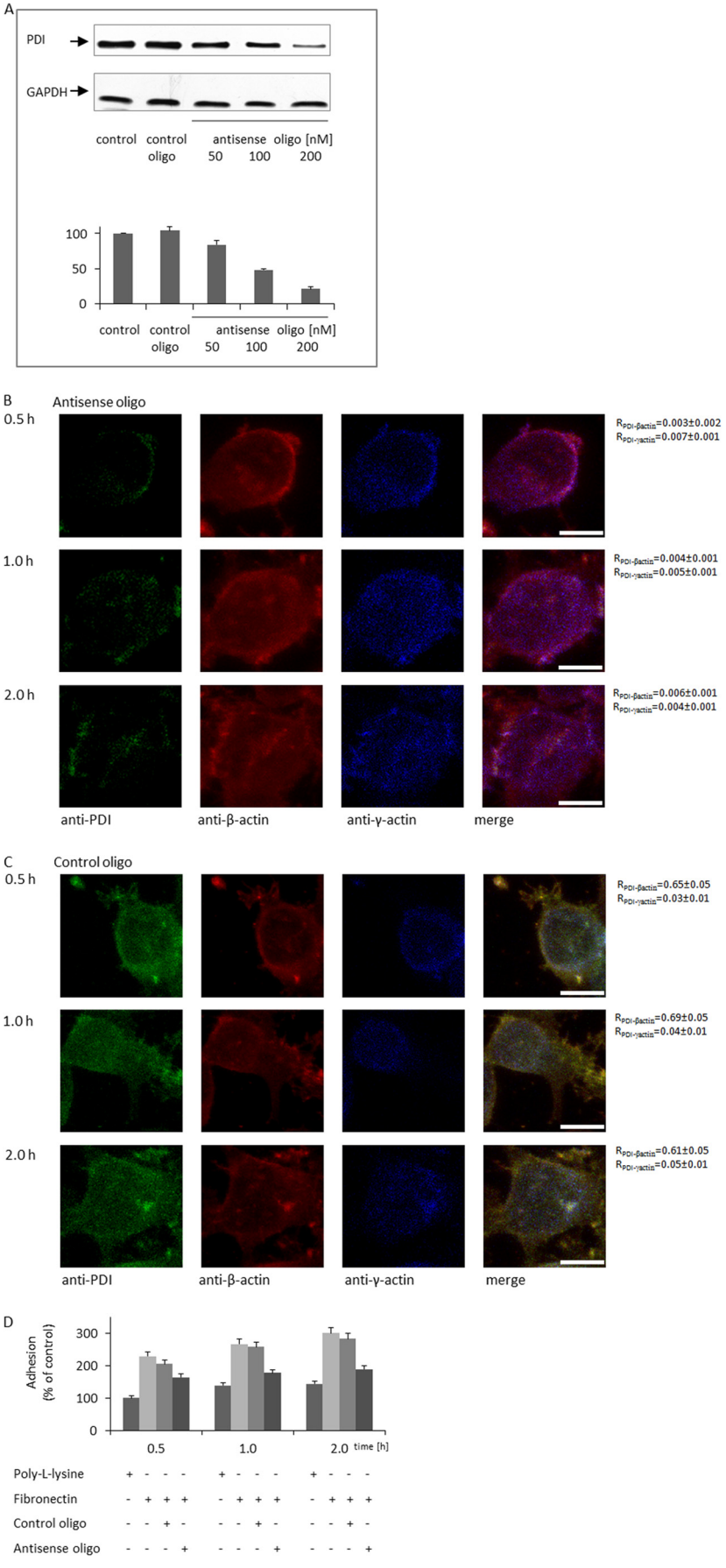
A
PDI
GAPDH
control
control oligo
antisense oligo 50
oligo 100
oligo [nM] 200
100
50
0
B
Antisense oligo
0.5 h
1.0 h
2.0 h
$R_{PDI-\beta actin}$=0.003±0.002
$R_{PDI-\gamma actin}$=0.007±0.001
$R_{PDI-\beta actin}$=0.004±0.001
$R_{PDI-\gamma actin}$=0.005±0.001
$R_{PDI-\beta actin}$=0.006±0.001
$R_{PDI-\gamma actin}$=0.004±0.001
anti-PDI
anti-β-actin
anti-γ-actin
merge
C
Control oligo
0.5 h
1.0 h
2.0 h
$R_{PDI-\beta actin}$=0.65±0.05
$R_{PDI-\gamma actin}$=0.03±0.01
$R_{PDI-\beta actin}$=0.69±0.05
$R_{PDI-\gamma actin}$=0.04±0.01
$R_{PDI-\beta actin}$=0.61±0.05
$R_{PDI-\gamma actin}$=0.05±0.01
anti-PDI
anti-β-actin
anti-γ-actin
merge
D
Adhesion (% of control)
300
200
100
0
0.5
1.0
2.0 time [h]
Poly-L-lysine
Fibronectin
Control oligo
Antisense oligo

nal antibody to γ-actin-CYA indicated that PDI is not able to interact with γ-actin (Fig. 1*D*, *right panel*). The results (Fig. 1*D*) suggest that PDI is able to bind only to β-actin and that this interaction is dependent on the time of adhesion. The observed interaction was rapidly increasing during the first hour of adhesion (~173% in comparison to zero time point) and then decreased slowly during the second one. Next, interaction of both proteins was tested in the cytoplasmic fraction (Fig. 1*E*). For this purpose the cytoplasmic fraction was isolated under mild conditions using NE-PER nuclear and cytoplasmic extraction reagents to obtain nondenatured, active proteins. Then PDI was immunoprecipitated by polyclonal anti-PDI antibodies and separated by SDS-PAGE in 10% gels under nonreducing and reducing conditions. Blotting with a monoclonal antibody to β-actin-CYA showed that PDI is associated with β-actin in the cytoplasm as well. Their interaction, as in the whole cell lysate, reached the highest level after an hour of cell adhesion and then decreased during the second hour. To control the protein concentration in each cell extract, before immunoprecipitation they were analyzed by Western immunoblotting using anti-β-actin-CYA, anti-PDI, and anti-GAPDH antibodies. Finally, to determine the subcellular distribution of PDI and its colocalization with β-actin, MEG-01 cells adhering to fibronectin were stained with antibodies that specifically recognize these proteins and were then examined by immunofluorescence (Fig. 1*F*). To detect PDI, the cells were treated with a polyclonalanti-PDI-TRITC antibody. Then the cells were stained with monoclonal anti-β-actin-CYA conjugated with FITC and anti-γ-actin-CYA conjugated with CY5.5 antibodies. PDI was found in the whole cytoplasm by showing strong punctuate staining together with a diffuse cytoplasmic localization. The average fluorescence derived from PDI and β-actin when merged revealed perimembrane regions with colocalization of both proteins, especially in the area of cell adhesion and spreading (Fig. 1*F*). The observed changes in the intensity of interaction between β-actin and PDI, and particularly strong colocalization of the examined proteins in the lamellipodial protrusions, suggested that there was participation of PDI in the regulation of cell adhesion, whereas colocalization between γ-actin and PDI was very poor. The colocalization was confirmed by calculating the Mander coefficient, which amounted to 0.63 ± 0.06, 0.74 ± 0.03, and 0.67 ± 0.06 for β-actin and PDI and 0.21 ± 0.02, 0.24 ± 0.03, and 0.23 ± 0.03 for γ-actin and PDI after 0.5, 1.0, and 2.0 h of cell adhesion, respectively. Moreover, Forester resonance energy was calculated. These examinations showed that marked levels of energy transfer occurred exclusively between β-actin and PDI. This process is clearly illustrated in Fig. 1*F*, where the estimated energy transfer efficiency value between both tested proteins was appreciably high (E_{eff} = ~40%). FRET confirmed that direct protein interaction between γ-actin and PDI did not take place (Fig. 1*F*). The E_{eff} was very low (1.4–1.7%).

We applied an antisense strategy to further evidence the role of PDI in actin cytoskeleton reorganization during cell adhesion. Incubation of MEG-01 cells with 50, 100, and 200 nM of antisense oligonucleotides specific to PDI mRNA efficiently and specifically down-regulated expression of this protein, as is shown by SDS-PAGE and blotting with monoclonal anti-PDI antibodies (Fig. 2*A*). After scanning these gels, it appeared that antisense oligonucleotide reduced the expression of PDI in a concentration-dependent manner which, at a concentration of 200 nM, caused ~70% inhibition when compared with the control oligonucleotide with a scrambled sequence. Consistently, when such cells were analyzed by confocal microscopy, they clearly showed a lack of colocalization of PDI with β-actin or γ-actin (Fig. 2*B*). The calculated Mander coefficient was very low and ranged from 0.003 ± 0.001 to 0.007 ± 0.001. Down-regulation of PDI in MEG-01 radically delayed their spreading onto the fibronectin. 2 h after seeding, they started changing their shape from circular to flattened with some pseudopodia. Treatment with control oligonucleotide did not affect PDI expression in the MEG-01 cells and had no effect on adhesion and spreading of cells (Fig. 2*C*). These cells showed numerous lamellipodial protrusions. Colocalization of PDI with β-actin and γ-actin was detectable, and the Mander coefficient value was not different from those observed in the control cells.

MEG-01 cells with reduced PDI expression showed extensively diminished adhesion to fibronectin (Fig. 2*D*). In this experiment, the adhesion of cells transfected with control or antisense oligonucleotides to PDI was studied by using dishes coated with fibronectin or poly-L-lysine.

β-Actin Cys^{374} Is Directly Involved in Interaction with PDI—In the preliminary experiments, to evaluate the role of free thiol groups in the interaction of PDI with β-actin, MEG-01 cells adhering to fibronectin were treated with *N*-ethylmaleimide (NEM), then lysed, and used in immunoprecipitation experiments. PDI was precipitated with specific antibodies, separated by SDS-PAGE, and tested by Western immunoblotting with the anti-β-actin antibody. Fig. 3*A* shows that treatment of MEG-01 cells with NEM dramatically reduced the amount of β-actin coimmunoprecipitated with PDI, thus indicating that these proteins poorly interact in the cellular fraction of NEM-treated cells adhering to fibronectin. The lowest panel shows concentrations of β-actin, PDI, and GAPDH before the experiment in cell lysates tested by Western immunoblotting. This observation was further confirmed by confocal microscopy analysis

FIGURE 2. **Down-regulation of PDI expression in MEG-01 cells with antisense oligonucleotide abolishes cell adhesion and spreading on fibronectin.** MEG-01 cells were preincubated with antisense (*Antisense oligo*) or control oligonucleotides (*Control oligo*) with a scrambled sequence. *A*, expression of PDI was evaluated by Western immunoblotting (*WB*) using monoclonal anti-PDI antibodies in comparison to nontreated (control) cells. *B* and *C*, adhering MEG-01 cells treated with antisense (*B*) or control (*C*) oligonucleotides were then analyzed by confocal microscopy. The cells were labeled by anti-PDI and anti-β-actin-CYA and anti-γ-actin-CYA antibodies conjugated with FITC and TRITC and Cy5.5, respectively. Colocalization of appropriate proteins was marked by *white points* in the *enlarged sections*, as shown in the control cells, and there was no colocalization detectable in cells treated with antisense oligonucleotides. Cell images are representative of more than 50 cells analyzed during three independent experiments. The Mander coefficient (*R*) was calculated from at least 20 confocal sections by Leica confocal software. Finally, adhesion of MEG-01 cells with down-regulated PDI expression was evaluated after 0.0–2.0 h of incubation with the use of fibronectin-coated 96-well plates. The number of adherent cells was determined using the CyQuant proliferation assay kit (Invitrogen). *D*, as a control, nontreated cells adherent to fibronectin and to poly-L-lysine were used. The data are presented as means ± S.D. obtained during three independent experiments and using adhesion to poly-L-lysine as a control.

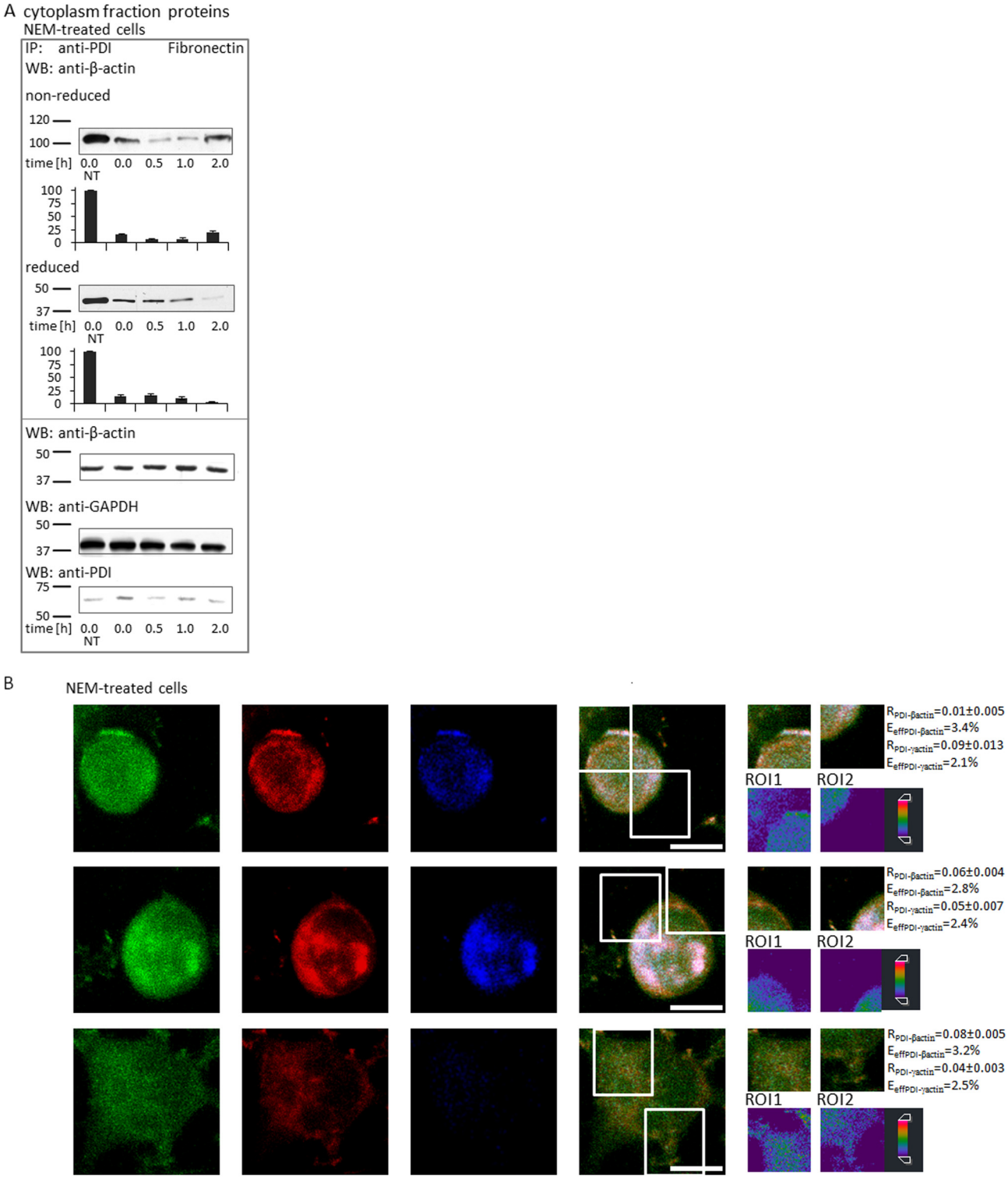

FIGURE 3. **Effect of *N*-ethylmaleimide on the interaction of PDI with β-actin.** MEG-01 cells pretreated with *N*-ethylmaleimide were placed on fibronectin for 0.0, 0.5, 1.0, and 2.0 h. *A*, then the MEG-01 cells were fractioned, and the cytosol fraction was subjected to immunoprecipitation (*IP*) with rabbit anti-PDI antibodies followed by blotting with a monoclonal anti-β-actin-CYA antibody. The *top* and *middle gels* show protein bands obtained under nonreducing and reducing conditions, respectively. In addition, the levels of β-actin and GAPDH and PDI in each sample before immunoprecipitation were tested by Western immunoblotting (*WB*) using rabbit anti-β-actin, mouse anti-GAPDH, and anti-PDI antibodies (*bottom gels*). The data are representative of three independent experiments. The same MEG-01 cells were stained with anti-PDI and anti-β-actin-CYA and anti-γ-actin-CYA antibodies and analyzed by confocal microscopy. *B*, a lack of colocalization of both proteins in MEG-01 cells pretreated with NEM to block free thiol groups (*enlarged sections*). The images are representative of more than 50 cells observed in three independent experiments. The Mander coefficient (*R*) was calculated from at least 20 confocal sections by Leica confocal software. FRET analysis confirmed a lack of interaction between tested proteins. The increase of fluorescence intensity is converted to pseudocolor (*right panel*) that displays variations of pixel gray scales with color.

(Fig. 3*B*). MEG-01 cells in which free thiols were blocked by NEM when placed on fibronectin essentially displayed the morphology of control cells adhering to poly-L-lysine. They were characterized by a disorganized actin cytoskeleton and a rounded shape, thus indicating that blocking free thiols inhibited the formation of lamellipodial extensions and effectively

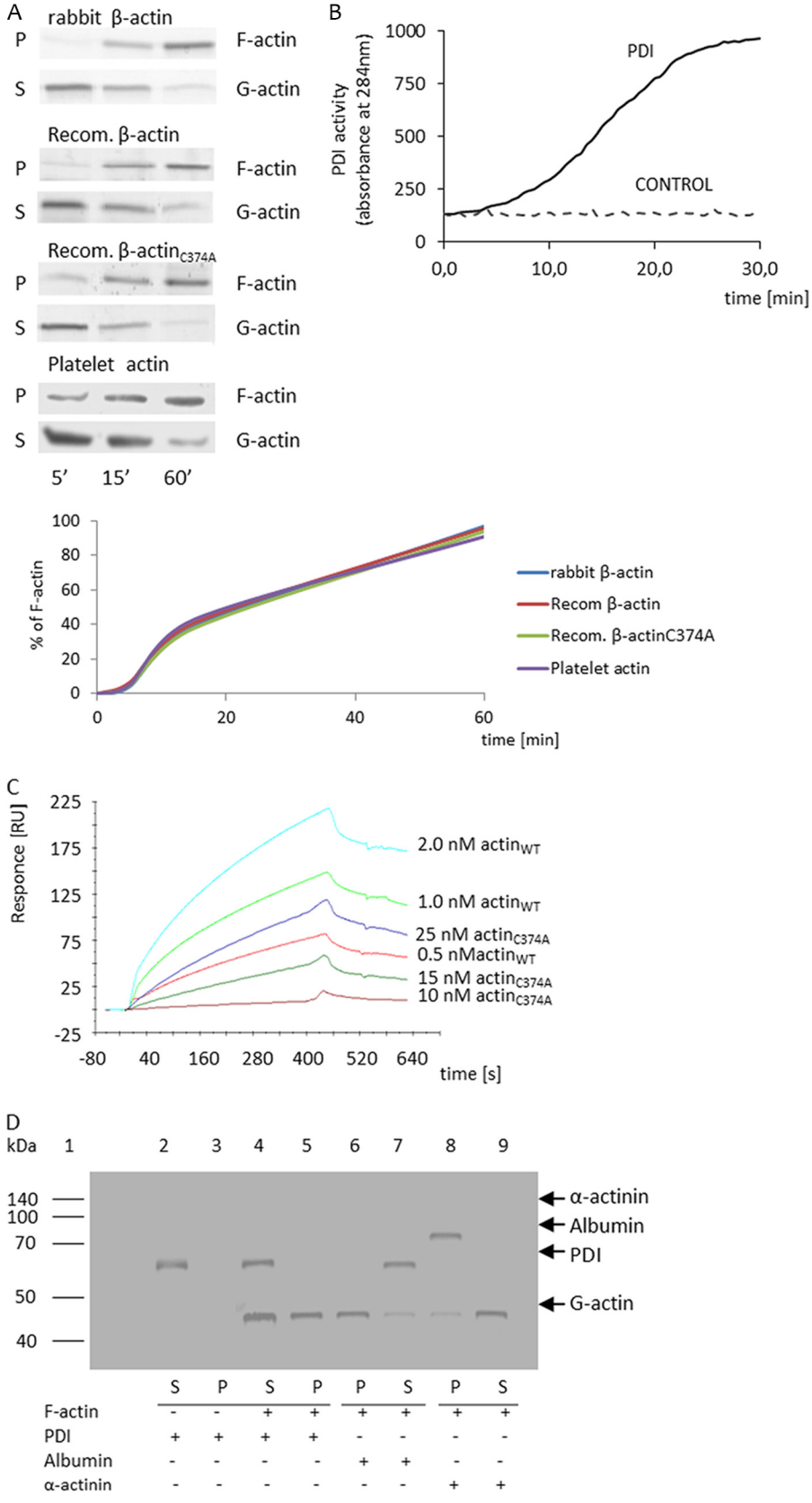

abolished colocalization of PDI and β-actin and γ-actin (Fig. 3*A*). Additionally, the Mander coefficient value was very low (between 0.01 and 0.09), which confirmed the lack of colocalization between these proteins. Moreover FRET analysis showed lack of interaction between PDI and β-actin-CYA as well as between PDI and γ-actin-CYA (E_{eff} of ~3.0 and 2.0%, respectively). At the beginning of adhesion, interaction between the β-actin-PDI complex and the proteins was very low (~6% in comparison to the control, nontreated cells) and remained practically unaltered for the whole time of the experiment (Fig. 3*B*).

Because this assay had low specificity in the next series of experiments, we focused on the role of the free thiols that were present in the β-actin molecule during interaction with PDI. Recent studies indicated that β-actin Cys^{374} is glutathionylated and that this modification is essential for cell spreading and cytoskeleton reorganization (2). Therefore, to determine whether β-actin Cys^{374} is involved in complexing with PDI, recombinant PDI, β-actin, and its mutant β-$actin_{C374A}$ were expressed in *E. coli* and purified to homogeneity. Next, their ability to polymerize was compared with that of control rabbit β-actin (Fig. 4*A*). Representative gel images showing F-actin- and G-actin band intensities for commercial rabbit β-actin, recombinant β-actin and its mutant (β-$actin_{C374A}$) formed after 5, 15, and 60 min, respectively, are illustrated in Fig. 4*A*. As is clearly shown, recombinant β-actin and its mutant demonstrated the same efficiency to form F-actin as that of control rabbit β-actin in the actin-binding protein buffer. No significant effects were observed in the absence of the polymerization buffer (not shown). Furthermore, they showed the same kinetics of polymerization. Fig. 4*B* shows that the recombinant PDI used in this experiment was enzymatically active, as evidenced by its ability to renaturate ribonuclease. Real time biomolecular interactions during complex formation between purified PDI and recombinant β-actin or its mutant were then monitored by surface plasmon resonance analysis. For this purpose, limiting amounts of PDI were immobilized on sensor chips through amine coupling. The obtained sensograms describing the binding of β-actin to immobilized PDI showed a typical association stage but a disturbed dissociation stage, thus indicating that the initial reversible interaction of both proteins became an irreversible one (Fig. 4*C*). The values of the association constants calculated for the reversible interaction of β-actin with PDI showed a value of K_D equal to 5.95×10^{-10}. There was no binding of β-actin to the uncoated surface or to the immobilized albumin used as a control protein. When β-$actin_{C374A}$ was used in place of β-actin, there was essentially no interaction detectable with PDI, thus indicating that this residue plays a critical role in interaction with the PDI molecule (Table 1).

TABLE 1

Rate constants for binding of PDI to β-actin

PDI was covalently immobilized on a BIAcore CM5 sensor chip (ΔRU = 2000). The analyte was injected at 25 °C, and binding was followed over time by the change in RU. The k_{on} and k_{off} values were determined from the association and dissociation phase, respectively, with three different concentrations of actin or its Cys^{374} mutant. The apparent K_D corresponds to the k_{off}/k_{on} ratio.

No.	PDI complex with	k_{on} ± S.E.	k_{off} ± S.E.	K_D ± S.E.
		$10^5 \cdot M^{-1} \cdot s^{-1}$	s^{-1}	M
1	β-Actin	9.37 ± 1.1	$5.57 \pm 0.43 \times 10^{-4}$	5.95×10^{-10}
2	β-$Actin_{C374A}$	2.15 ± 0.9	$2.34 \pm 0.38 \times 10^{-2}$	1.09×10^{-7}

To test whether PDI can interact with F-actin, initially cosedimentation assay with commercial available rabbit actin was made (Fig. 4*D*). It revealed that PDI (*lanes 2–5*) was located in the soluble fraction after centrifugation both in the absence and in the presence of actin. α-Actinin, a known actin-binding protein, was used as a positive control and pelleted with actin (*lanes 8* and *9*), whereas BSA, known as non-actin-binding protein, was used as a negative control and remained only in the soluble fraction (*lanes 6* and *7*). The obtained results suggested that PDI preferentially interacted with globular actin (*G-actin*).

To further examine whether the mutation of β-actin Cys^{374} affects complex formation with PDI, the MEG-01 cells were transfected with pEGFPN1 expressing β-actin or its mutated form, in which cysteine was replaced by alanine (pEGFP-N1-$actin_{C374A}$). First, we attempted to evaluate the expression of EGFP proteins after transfection of MEG-01 cells (Fig. 5*A*). Western immunoblotting of pEGFP-N1-β-actin and pEGFP-N1-β-$actin_{C374A}$ after separation of the cell lysates by SDS-PAGE showed an additional band with a molecular mass of ~75 kDa corresponding to β-actin linked to EGFP. Densitometric scanning of the blots and quantification of the expressed proteins showed that EGFP-β-actin and EGFP-β-$actin_{C374A}$ corresponded to ~50% of total cell β-actin. Then after plating the cells on fibronectin and incubation for 0–2.0 h, the cells were lysed and used in immunoprecipitation experiments with anti-PDI antibodies (Fig. 5*B*). Western immunoblotting with anti-β-actin antibodies showed a dramatic decrease in the intensity of the protein band with a molecular mass of 110 kDa that was immunoprecipitated from cells transfected with pEGFP-β-$actin_{C374A}$, when compared with that containing control pEGFP-β-actin. Consistently, the immunoprecipitate produced by the anti-PDI antibodies contained significantly less

FIGURE 4. **PDI binds to G-actin dependent on the Cys^{374} residue.** *A*, the ability of recombinant wild type β-actin and its mutant β-$actin_{C374A}$, platelet actin to polymerize skeletal muscle actin was compared with that of muscle β-actin (Rb). G-actins were polymerized during 5, 15, or 60 min and separated to the supernatant (*S*) and pellet (*P*) fractions, respectively. Equal volume samples (15 μl) were prepared with sample buffer and separated by SDS-PAGE in 12% polyacrylamide gels. The gels were scanned, and the protein bands were quantitated using the Gel Doc 2000 gel documentation system (Bio-Rad). The results of these analyses are shown by plotting the amount of F-actin on the duration of time polymerization. As a control, experiments without the polymerization buffer were carried out (data not shown). *B*, the activity of recombinant PDI was assayed by measuring the renaturation of RNase, which was monitored by measuring absorbance at 284 nm using a Unicam UV-visible spectrophotometer. Interaction of purified recombinant β-actin and its mutant β-$actin_{C374A}$ with active recombinant PDI was tested by surface plasmon resonance. For this purpose, recombinant PDI was immobilized on a sensor chip CM5. *C*, 5-μl aliquots of β-actin or β-$actin_{C374A}$ solutions with a concentration ranging from 10 to 25 nM were injected, and the complex formation was monitored at a flow rate of 5 μl/min. In parallel, a BSA solution was injected at the same flow rate as a control protein (not shown). *D*, a cosedimentation assay was performed to evaluate whether PDI can interact with F-actin. PDI, α-actinin, and BSA were incubated with or without F-actin and centrifuged at 16,000 × *g* for 60 min. Subsequently, pellets (*P*) and supernatants (*S*) were analyzed by SDS-PAGE in 12% gels. PDI bound to G-actin was indicated by its presence in the actin supernatant after centrifugation. Control BSA did not cosediment, whereas α-actinin was interacting with F-actin. These data are representative of three independent experiments. *RU*, resonance units.

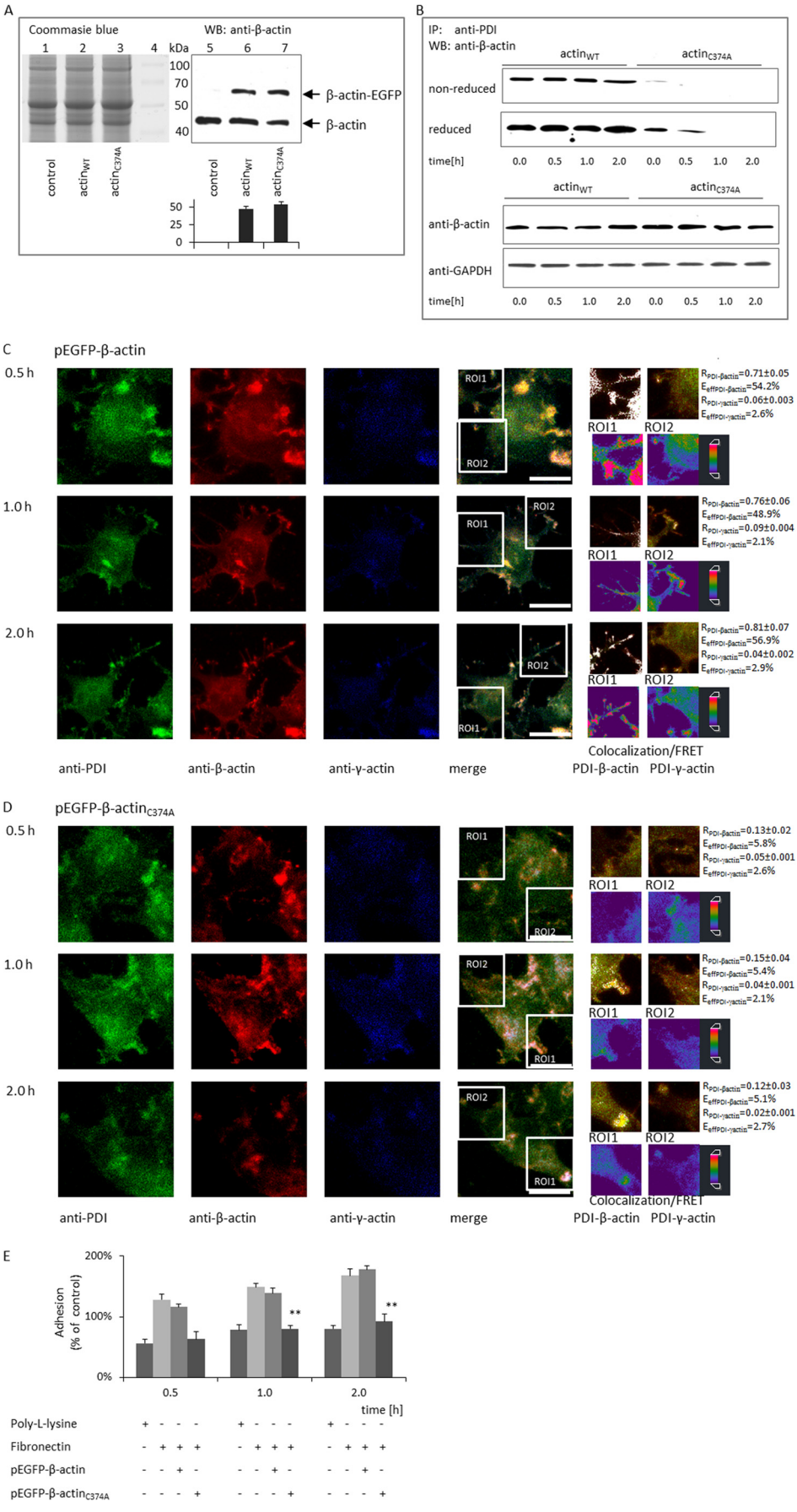
A
Coommasie blue
WB: anti-β-actin
1 2 3 4 kDa 5 6 7
100
70
50
40
β-actin-EGFP
β-actin
control
actinWT
actinC374A
50
25
0
B
IP: anti-PDI
WB: anti-β-actin
actinWT
actinC374A
non-reduced
reduced
time[h]
0.0 0.5 1.0 2.0 0.0 0.5 1.0 2.0
anti-β-actin
anti-GAPDH
C
pEGFP-β-actin
0.5 h
1.0 h
2.0 h
ROI1
ROI2
RPDI-βactin=0.71±0.05
EeffPDI-βactin=54.2%
RPDI-γactin=0.06±0.003
EeffPDI-γactin=2.6%
RPDI-βactin=0.76±0.06
EeffPDI-βactin=48.9%
RPDI-γactin=0.09±0.004
EeffPDI-γactin=2.1%
RPDI-βactin=0.81±0.07
EeffPDI-βactin=56.9%
RPDI-γactin=0.04±0.002
EeffPDI-γactin=2.9%
anti-PDI
anti-β-actin
anti-γ-actin
merge
Colocalization/FRET
PDI-β-actin
PDI-γ-actin
D
pEGFP-β-actinC374A
RPDI-βactin=0.13±0.02
EeffPDI-βactin=5.8%
RPDI-γactin=0.05±0.001
EeffPDI-γactin=2.6%
RPDI-βactin=0.15±0.04
EeffPDI-βactin=5.4%
RPDI-γactin=0.04±0.001
EeffPDI-γactin=2.1%
RPDI-βactin=0.12±0.03
EeffPDI-βactin=5.1%
RPDI-γactin=0.02±0.001
EeffPDI-γactin=2.7%
E
Adhesion (% of control)
200%
100%
0%
0.5
1.0
2.0
time [h]
**
Poly-L-lysine
Fibronectin
pEGFP-β-actin
pEGFP-β-actinC374A

β-actin when we used MEG-01 cells transfected with pEGFP-β-actin$_{C374A}$. Then we switched to confocal microscopy again to explore the impact of β-actin Cys^{374} on cell adhesion and spreading that was observed at the level of a single cell. In typical experiments, the MEG-01 cells were transfected with pEGFP-β-actin or pEGFP-β-actin$_{C374A}$ by using Lipofectamine, respectively. They were placed on fibronectin and incubated for up to 2 h, then fixed with paraformaldehyde, and counterstained with anti-PDI-TRITC and anti-γ-CYA antibodies labeled by Cy5.5. Cells transfected with GFP-tagged β-actin (Fig. 5*C*) or β-actin$_{C374A}$ (Fig. 5*D*) showed much higher expression of the fluorescently labeled intact β-actin. Its distribution matched that of the endogenous β-actin (Fig. 5*C*), it showed much higher accumulation in the cytoplasm and was close to the membranes. There were heavy accumulations of GFP-tagged β-actin at the lamellar protrusions, and overlapping staining of PDI seen as white points was particularly evident
at these sites. In contrast, MEG-01 cells transfected with pEGFP-β actin$_{C374A}$ exhibited a round morphology and an impaired actin cytoskeleton organization (Fig. 5*D*), similar to that observed in cells treated with *N*-ethylmaleimide (Fig. 3*A*). Colocalization of PDI and site-mutated actin$_{C374A}$ was significantly lower than that observed in the control cells or in the pEGFP-β-actin-transfected cells. Furthermore, cells transfected with pEGFP-β-actin$_{C374A}$ adhered much less efficiently and showed impaired spreading on the fibronectin-coated slides. Interaction between PDI and γ-actin-CYA was very low like in the control cells. FRET method confirmed strong interaction between pEGFP-β-actin and PDI lack of interaction between pEGFP-β-actin$_{C374A}$ and PDI (E_{eff} between 50–54% and ~6%, respectively). Fig. 5*E* shows adhesion of the transfected MEG-01 cells to fibronectin and poly-L-lysine. Transfection of the MEG-01 cells with pEGFP-β-actin$_{C374A}$ significantly reduced adhesion to fibronectin when compared with the control cells or cells transfected with pEGFP-β-actin. The adhering cells were quantitated by means of CyQUANT (Molecular Probes) using the Wallac VICTOR 1420 multilabel counter (PerkinElmer Life Sciences).

αIIbβ3 Is Essential for Interaction of PDI with β-Actin—To examine whether αIIbβ3, a major integrin receptor of MEG-01, is implicated in the interaction of PDI with β-actin, in subsequent experiments the cells were preincubated with RGD peptide or anti-αIIbβ3 monoclonal antibodies, placed on fibronectin, and analyzed in terms of colocalization of both proteins. Control MEG-01 cells treated with RGE peptide or normal mouse IgG showed a typical morphology of adhering cells with numerous lamellipodial protrusions and efficient colocalization of PDI with β-actin (Fig. 6*A*). Treatment of cells with the RGD peptide or anti-αIIbβ3 abolished the β-actin-PDI complex formation (Fig. 6, *B* and *C*). Such cells displayed a rounded shape with a disorganized peripheric actin cytoskeleton. However, after 2 h they started to spread and showed the appearance of pseudopodia. All those experiments were confirmed by FRET analysis.

DISCUSSION

Cell adhesion and motility play key roles in a variety of biological processes, including angiogenesis, inflammation, and wound healing. Both adhesion and motility involve the expansion of the plasma membrane, which takes place through the formation of either thin actin-rich protrusions called lamellipodia or finger-like projections known as filopodia. Variations in the rate of expansion may have striking effects on the course of numerous phenomena. The formation of both lamellipodia and filopodia engages the polymerization of actin filaments.

The data presented here demonstrate that PDI interacts exclusively with β-actin-CYA during integrin-mediated cell adhesion to fibronectin and that it promotes cytoskeleton reorganization. Specifically, we provided evidence that: (*a*) both proteins can directly interact in a purified system, as is documented by solid phase binding assay and surface plasmon resonance analysis; (*b*) PDI preferentially binds to G-actin; (*c*) intracellularly PDI and β-actin form a complex with a molecular mass of 110 kDa that can be immunoprecipitated with specific antibodies either to PDI or β-actin; the complex dissociates upon reduction; β-actin Cys^{374} is involved in the creation of a disulfide bond with PDI and is responsible for integrity of the β-actin-PDI complex; mutation of the Cys^{374} residue abolishes the ability of β-actin to interact with PDI; (*d*) PDI colocalizes with β-actin in adhering MEG-01 cells and predominantly in areas close to the membrane in the lamellipodial protrusions; (*e*) down-regulation of PDI expression with antisense oligonucleotide abolishes adhesion of the MEG-01 cells to fibronectin

FIGURE 5. **The β-actin Cys^{374} residue is directly involved in interaction with PDI during cell adhesion to fibronectin.** To evaluate the expression of EGFP-β-actin$_{WT}$ or its mutant EGFP-β-actin$_{C374A}$ after the transfection of MEG-01 cells, Western immunoblotting (*WB*) with an antibody specific to β-actin was performed. *A*, the quantity of endo- and exogenous β-actin is shown below the corresponding gels. For this purpose, after immunodetection using the enhanced chemiluminescence kit, the films were scanned, and the protein bands were quantitated using the Gel Doc 2000 gel documentation system (Bio-Rad). The background was subtracted, and the area for each protein peak was determined. In parallel, samples of cell extract were blotted with control mouse IgG (data not shown). *B*, next, MEG-01 cells transfected with pEGFP-β-actin or its mutant pEGFP-β-actin$_{C374A}$ were subjected to immunoprecipitation (*IP*) with rabbit polyclonal anti-PDI antibody, separated by SDS-PAGE under nonreducing and reducing conditions, and blotted with monoclonal anti-β-actin-CYA antibody (*upper gels*). In parallel, samples of cell extracts used in the immunoprecipitation experiments were analyzed by Western immunoblotting by using monoclonal anti-β-actin or anti-GAPDH antibodies (*lower gels*). The blots are representative of three independent experiments. *C*, the adhesion of control MEG-01 cells, transfected with pEGFP-β-actin or pEGFP-β-actin$_{C374A}$, to fibronectin. Cells were added to fibronectin-coated 96-well plates, and the number of adherent cells after 0.5, 1.0, and 2.0 h of incubation was determined with the CyQuant proliferation assay Kit (Invitrogen). Nontreated cells adherent to poly-L-lysine were used as a control. The data are presented as means ± S.D. obtained during three independent experiments. *D* and *E*, MEG-01 cells transfected with pEGFP-β-actin or pEGFP-β-actin$_{C374A}$ and analyzed by confocal microscopy. MEG-01 cells after transfection were placed on fibronectin for 0.5, 1.0, or 2.0 h, and then they were fixed, permeabilized, and treated with rabbit antibodies specific to PDI-conjugated TRITC and anti-γ-actin-CYA-Cy5.5 antibody. The enlarged sections show colocalization of both proteins in MEG-01 cells transfected with pEGFP-β-actin and the lack of colocalization when the cells were transfected with pEGFP-β-actin$_{C374A}$. The pictures are representative of more than 50 cells observed during three independent experiments. The Mander coefficient (*R*) was calculated from at least 20 confocal sections by Leica confocal software. FRET analysis showed strong interaction between β-actin-CYA and PDI, whereas γ-actin practically did not bind to PDI. The increase of fluorescence intensity is converted to pseudocolor (*right panel*) that displays variations of pixel gray scales with color.

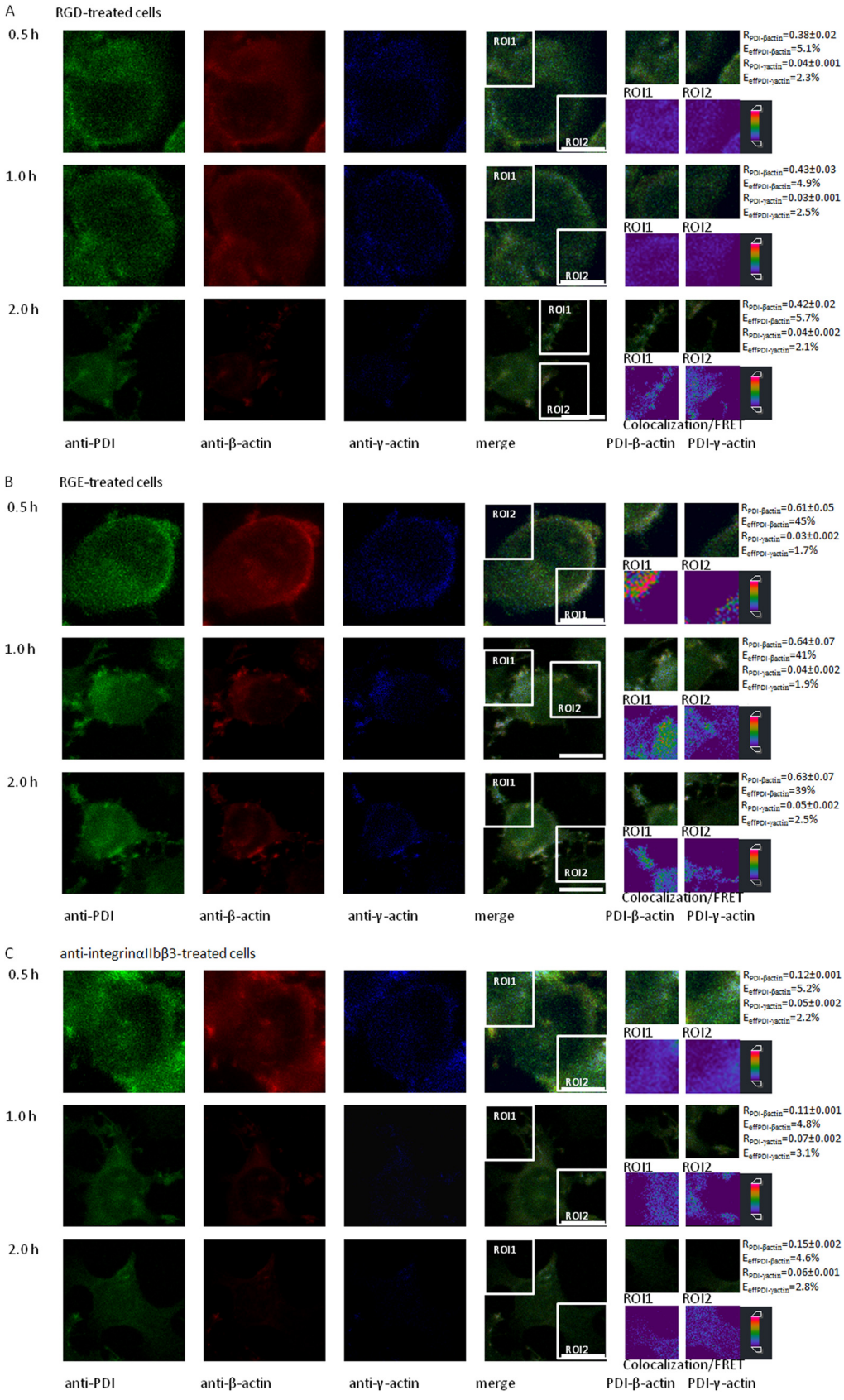

FIGURE 6. **Interaction of PDI with β-actin in adhering MEG-01 cells depends on αIIbβ3.** *A–C*, MEG-01 cells were incubated with RGD (*A*), RGE (*B*), and anti-αIIbβ3 antibodies (*C*) and placed on fibronectin for 0.5, 1.0, and 2.0 h. Then the cells were fixed, permeabilized, and labeled with specific antibodies to PDI and β-actin, as described in the legend to Fig. 1. Localization and colocalization of the tested protein was analyzed under a Leica TCS SP5 confocal microscope. Cell images are representative of more than 50 cells observed during three independent experiments. The Mander coefficient (*R*) was calculated from at least 20 confocal sections by Leica confocal software. FRET analysis was made as previously described.

and appreciably delays their spreading; and (*f*) the binding of PDI to β-actin in the adhering cells requires the functionally active αIIbβ3 integrin. Treatment of the cells with the RGD peptide or anti-αIIbβ3 antibodies prevents colocalization of PDI with β-actin.

By using specific monoclonal antibody, we showed that PDI directly interact only with β-actin isoform but not with γ-actin during adhesion. These two isoforms of actin display distinct distribution and different functional roles and participate differently in organization of cell morphology, polarity, and motility. β-Actin is preferentially localized in stress fiber, in circular bundles, and at cell-cell contacts, suggesting its role in cell attachment. The crucial role for γ-actin is control of cell motility (23). Our previous work showed that PDI is able to interact with integrin (16). It is possible that PDI is recruited to the adhesion area by active form of integrin αIIbβ3, therefore interacting with β-actin in these compartments during cell adhesion and spreading. However, this supposition requires further investigations.

Recent observations indicate that reactive oxygen species that are produced during processes occurring in the ECM, for example, by adhering cells, modify the structure of cytoskeletal proteins, cause cytoskeleton reorganization, and weaken cell spreading (2). Oxidation of cysteine residues resulting from integrin-dependent transmembrane signaling seems to be a key mechanism in the regulation of the β-actin function. During cell adhesion, β-actin Cys^{374} was described to be directly modified by the formation of a disulfide bond with reduced glutathione (2). *S*-Glutathionylation of this residue is induced by oxidative stress (24). Interestingly, β-actin undergoes reversible *S*-glutathionylation in response to stimulation by the epidermal growth factor. Deglutathionylation of G-actin leads to an ~6-fold increase in the rate of polymerization and the F-actin content. F-actin was found in the cell periphery, which suggests that actin polymerization is regulated by a mechanism of reversible glutathionylation (25). *S*-Glutathionylation is reversible in either an enzyme-dependent or -independent manner. The principle enzyme that removes glutathione from the mixed sulfides is glutaredoxin, although thioredoxin or protein disulfide isomerase can also catalyze this reaction (26, 27). In other systems, PDI showed lower deglutathionylation activity when compared with glutaredoxin; however, in contrast to glutaredoxin, only PDI could create the mixed disulfide intermediate (28). Furthermore, PDI is able to form native disulfide bonds in fully glutathionylated protein substrates (29, 30).

Our data showed that β-actin Cys^{374} constitutes the binding site for PDI in cells adhering to ECM after its translocation from endoplasmic reticulum compartments toward the cytosol in response to integrin engagement. Such translocation of PDI to the cytosol was observed after activation of human neutrophils by phorbol ester (31). The disulfide-bonded complex between PDI and β-actin may provide a mechanism that protects cells against irreversible cytoskeleton reorganization. It was reported that oxidation of β-actin Cys^{374} destabilizes intermonomer interactions of β-actin (6). On the other hand, reactive oxygen species are known to interfere with the organization of actin microfilaments and motility of many eukaryotic cells (32). Therefore, oxidation of Cys^{374} could be critical for the disassembly of filaments, when the environment is more oxidative because of a shifted GSH/GSSH equilibrium (6).

The formation of disulfide bonds between β-actin monomers may be fundamental during cellular redox responses to growth factors or integrin stimulation. Then the resulting β-actin dimmers can be incorporated into F-actin during polymerization and can affect the cross-linking of F-actin and its elasticity (33). Our study suggests that PDI can be responsible for the disulfide-thiol exchange by providing the mechanism for the regulation of β-actin cytoskeleton rearrangement during cell adhesion.

To sum up, our data show that PDI can be an element of the mechanism leading toward cytoskeleton reorganization. It mediates the intramolecular disulfide-thiol rearrangement of β-actin in response to integrin engagement and forms a complex with β-actin Cys^{374}, which is localized in the focal adhesion plate mediating adhesion and cell spreading.

Acknowledgment—We gratefully acknowledge Professor Christine Chaponnier (Centre Medical Universitaire, Geneva, Switzerland) for anti-β-actin-CYA and anti-γ-actin-CYA antibodies.

REFERENCES

1. Hynes, R. O. (1992) Integrins. Versatility, modulation, and signaling in cell adhesion. *Cell* **69,** 11–25
2. Fiaschi, T., Cozzi, G., Raugei,G., Formigli, L., Ramponi, G., and Chiarugi, P. (2006) Redox regulation of β-actin during integrin-mediated cell adhesion. *J. Biol. Chem.* **281,** 22983–22991
3. Stournaras, C. (1990) Exposure of thiol groups and bound nucleotide in G-actin. Thiols as an indicator for the native state of actin. *Anticancer Res.* **10,** 1651–1659
4. Dalle-Donne, I., Giustarini, D., Rossi, R., Colombo, R., and Milzani, A. (2003) Reversible *S*-glutathionylation of C_{374} regulates actin filament formation by inducing structural changes in the actin molecule. *Free Radic. Biol. Med.* **34,** 23–32
5. Tsapara, A., Kardassis, D., Moustakas, A., Gravanis, A., and Stournaras, C. (1999) Expression and characterization of Cys^{374} mutated human β-actin in two different mammalian cell lines. Impaired microfilament organization and stability. *FEBS Lett.* **455,** 117–122
6. Lassing, I., Schmitzberger, F., Björnstedt, M., Holmgren, A., Nordlund, P., Schutt, C. E., and Lindberg, U. (2007) Molecular and structural basis for redox regulation of β-actin. *J. Mol. Biol.* **370,** 331–348
7. Hinshaw, D. B., Burger, J. M., Beals, T. F., Armstrong, B. C., and Hyslop P. A. (1991) Actin polymerization in cellular oxidant injury. *Arch. Biochem. Biophys.* **288,** 311–316
8. Omann, G. M., Harter, J. M., Burger, J. M., and Hinshaw D. B. (1994) H_2O_2-induced increased in cellular F-actin occur without increases in actin nucleation activity. *Arch. Biochem. Biophys.* **308,** 407–412
9. Gilbert, H. F. (1990) Molecular and cellular aspects of thiol-disulfide exchange. *Adv. Enzymol. Relat. Areas Mol. Biol.* **63,** 69–172
10. López-Mirabal, H. R., and Winther, J. R. (2008) Redox characteristics of the eukaryotic cytosol. *Biochim. Biophys. Acta* **1783,** 629–640
11. Noiva, R. (1999) Protein disulfide isomerase. The multifunctional redox chaperone of endoplasmic reticulum. *Semin. Cell Dev. Biol.* **10,** 481–493
12. Laurindo, F. R., Pescatore, L. A., and de Castro Fernandes, D. (2012) Protein disulfide isomerase in redox cell signaling and homeostasis. *Free Radic. Biol. Med.* **52,** 1954–1969
13. Essex, D. W., and Li, M. (2003) Redox control of platelet aggregation. *Biochemistry* **42,** 129–136
14. Jasuja, R., Furie, B., and Furie, B. C. (2010) Endothelium-derived but not platelet-derived protein disulfide isomerase is required for thrombus formation *in vivo*. *Blood* **116,** 4665–4674
15. Essex, D. W., Chen, K., and Swiatkowska, M. (1995) Localization of pro-

tein disulfide isomerase to the external surface of the platelet plasma membrane. *Blood* **86,** 2168–2173
16. Swiatkowska, M., Szymański, J., Padula, G., and Cierniewski, C. S. (2008) Interaction and functional association of protein disulfide isomerase with αVβ3 integrin on endothelial cells. *FEBS J.* **275,** 1813–1823
17. Farwell, A. P., Lynch, R. M., Okulicz, W. C., Comi, A. M., and Leonard, J. L. (1990) The actin cytoskeleton mediates the hormonally regulated translocation of type II Iodothyronine 5′-Deiodinase in astrocytes. *J. Biol. Chem.* **265,** 18546–18553
18. Safran, M., Farwell, A. P., and Leonard, J. L. (1992) Thyroid hormone-dependent redistribution of the 55-kilodalton monomer of protein disulfide isomerase in cultured glial cells. *Endocrinology* **131,** 2413–2418
19. Ogura, M., Morishima, Y., Ohno, R., Kato, Y., Hirabayashi, N., Nagura, H., and Saito, H. (1985) Establishment of a novel human megakaryoblastic leukemia cell line, MEG-01, with positive Philadelphia chromosome. *Blood* **66,** 1384–1392
20. Zai, A., Rudd, M. A., Scribner, A. W., and Loscalzo, J. (1999) Cell-surface protein disulfide isomerase catalyzes transnitrosation and regulates intracellular transfer of nitric oxide. *J. Clin. Invest.* **103,** 393–399
21. Thepparit, C., and Smith, D. R. (2004) Serotype-specific entry of dengue virus into liver cells. Identification of the 37-kilodalton/67-kilodalton high-affinity laminin receptor as a dengue virus serotype 1 receptor. *J. Virol.* **78,** 12647–12656
22. Towbin, H., Staehelin, T., and Gordon, J. (1979) Electrophoretic transfer of proteins from polyacrylamide gels to nitrocellulose sheets. Procedure and some applications. *Proc. Natl. Acad. Sci. U.S.A.* **76,** 4350–4354
23. Dugina, V., Zwaenepoel, I., Gabbiani, G., Clément, S., and Chaponnier, C. (2009) β- and γ-cytoplasmic actins display distint distribution and function diversity. *J. Cell Sci.* **122,** 2980–2988
24. Dalle-Donne, I., Giustarini, D., Colombo, R., Milzani, A., and Rossi, R. (2005) *S*-Glutathionylation in human platelets by a thiol-disulfide exchange-independent mechanism. *Free Radic. Biol. Med.* **38,** 1501–1510
25. Wang, J., Boja, E. S., Tan, W., Tekle, E., Fales, H. M., English, S., Mieyal, J. J., and Chock, P. B. (2001) Reversible glutathionylation regulates actin polymerization in A431 cells. *J. Biol. Chem.* **276,** 47763–47766
26. Dalle-Donne, I., Milzani, A., Gagliano, N., Colombo, R., Giustarini, D., and Rossi, R. (2008) Molecular mechanisms and potential clinical significance of *S*-glutathionylation. *Antioxid. Redox Signal.* **10,** 445–473
27. Reinhardt, C., von Brühl, M. L., Manukyan, D., Grahl, L., Lorenz, M., Altmann, B., Dlugai, S., Hess, S., Konrad, I., Orschiedt, L., Mackman, N., Ruddock, L., Massberg, S., and Engelmann, B. (2008) Protein disulfide isomerase acts as an injury response signal that enhances fibrin generation via tissue factor activation. *J. Clin. Invest.* **118,** 1110–1122
28. Peltoniemi, M. J., Karala, A. R., Jurvansuu, J. K., Kinnula, V. L., and Ruddock, L. W. (2006) Insights into deglutathionylation reactions. Different intermediates in the glutaredoxin and protein disulfide isomerase catalyzed reactions are defined by the gamma-linkage present in glutathione. *J. Biol. Chem.* **281,** 33107–33114
29. Ruoppolo, M., and Freedman, R. B. (1995) Refolding by disulfide isomerization. The mixed disulfide between ribonuclease T1 and glutathione as a model refolding substrate. *Biochemistry* **34,** 9380–9388
30. Ruoppolo, M., Freedman, R. B., Pucci, P., and Marino, G. (1996) Glutathione-dependent pathways of refolding of RNase T1 by oxidation and disulfide isomerization. Catalysis by protein disulfide isomerase. *Biochemistry* **35,** 13636–13646
31. Paes, A. M., Veríssimo-Filho, S., Guimarães, L. L., Silva, A. C., Takiuti, J. T., Santos, C. X., Janiszewski, M., Laurindo, F. R., and Lopes, L. R. (2011) Protein disulfide isomerase redox-dependent association with p47 (phox). Evidence for an organizer role in leukocyte NADPH oxidase activation. *J. Leukocyte Biol.* **90,** 799–810
32. Chiarugi, P., and Fiaschi, T. (2007) Redox signaling in anchorage-dependent cell growth. *Cell. Signal.* **19,** 672–682
33. Tang, J. X., Janmey, P. A., Stossel, T. P., and Ito, T. (1999) Thiol oxidation of actin produces dimmers that enhance the elasticity of the F-actin network. *Biophys. J.* **76,** 2208–2215